# Road Vehicle Detection and Classification Using Magnetic Field Measurement

Xiao Chen[1], Xiaoying Kong[1], Min Xu[1], Kumbesan Sandrasegaran[1], Jiangbin Zheng[2]
[1] Faculty of Engineering and Information Technology, University of Technology Sydney
[2] School of Software and Microelectronics, Northwestern Polytechnical University
Corresponding authors: Min Xu (min.xu@uts.edu.au), Jiangbin Zheng (zhengjb@nwpu.edu.cn)

***Abstract*—This paper presents a road vehicle recognition and classification approach for intelligent transportation systems. This approach uses a roadside installed low cost magnetometer and associated data collection system. The system measures the magnetic field changing, detects passing vehicles and recognizes vehicle types. We introduce Mel Frequency Cepstral Coefficients (MFCC) to analyze vehicle magnetic signals and extract it as vehicle feature with the representation of cepstrum, frame energy, and gap cepstrum of magnetic signals. We design a 3-dimensional map algorithm using Vector Quantization (VQ) to classify vehicle magnetic features to 4 typical types of vehicles in Australian suburbs: sedan, van, truck, and bus. In order to train an accurate classifier, training samples are selected using Dynamic Time Warping (DTW). Verification experiments show that our approach achieves a high level of accuracy for vehicle detection and classification.**

***Index Terms*—Vehicle Classification, Signal Processing, Road Traffic Model, Magnetic Sensing, Mel Frequency Cepstral Coefficients (MFCC), Vector Quantization (VQ), Dynamic Time Warping (DTW), Intelligent Transportation System (ITS)**

## I. Introduction

Intelligent transportation systems (ITS) apply sensors to collect and analyze road vehicle information for road vehicle monitoring and managing, control of road traffic, and traffic data analysis for future development of transportation infrastructures. Useful road traffic information includes: vehicle location, type, weight, passing speed and direction, and vehicle volume in certain zones [1, 2]. The first traffic monitor sensor was developed and installed for road use in 1928. This device used a microphone to detect vehicle sound [1]. Since then, road vehicle sensing technologies have been explored in vibration, inductive-loop detecting, magnetic field, acoustic sensing, optical and infrared sensing, satellite signal processing, camera captured image and video processing, and inertial sensing [1, 2]. These sensing technologies can be utilized for a single sensor, or in a sensor network.

Various types of sensing technologies can be applied in different locations in transportation systems. The sensors can be statically deployed on road side, underneath the road surface, over road, on a pole at an optimal height near the road, on bridge crossing over the road, or dynamically installed in road or aerial vehicles. In a sensor network, these technologies and deployment locations can be integrated.

From a commercial deployment perspective, the types of sensing technologies and the deployment locations of sensors will impact the reliability and cost of installation and maintenance. For example, magnetic sensor installation underneath the road surface will increase the sensor measurement accuracy, but disrupt the road traffic in installation and maintenance phases.

In this paper, we propose a road vehicle detection and classification approach using roadside-installed single magnetic sensor. The magnetic sensor measures the magnetic field changes when a vehicle is passing the sensor. The sensor measurement signals are analyzed to extract vehicle features, and these features are classified into vehicle types. Passing vehicles on road traffic are detected for four types of vehicles: sedan, van, truck, and bus.

This paper is organized as follows. Section II reviews related work in vehicle detecting and classification. Section III presents the experimental design for magnetic sensing in this research. Section IV presents an algorithm for vehicle identification and vehicle type classification. The results of the road vehicle identification and classification are demonstrated and evaluated in Section V. Conclusion are drawn finally in Section VI.

## II. Related Work

Sensing technologies provide vehicle and road traffic information to intelligent transportation systems.

Accelerometer is able to measure the vibration of the road when a vehicle is passing. ITS can receive sensor input from accelerometers installed under road surface, and compute the weight of passing vehicle and number of vehicles.

Inductive loop technology uses electrical conducting loop that is installed on road surface. When a vehicle passes the loop, a current is induced in wired loops, and this signal change is processed and transmitted to ITS to compute the detection of the passing vehicle type [1]. The vehicle detection and type classification algorithms include back-propagation neural networks [3], neural genetic controller using single-loop [4], and 2-axle tractor/3-axle semi-trailer approach [5].

Radar is a mature technology to detect passing vehicle length, height and speed. Frequency modulated continuous wave using doppler radar is one of the traditional radar techniques to extract shape information and classify vehicle types [6]. Recent radar techniques include detecting vehicle and analysis of the frequency of incoming vehicle and using reconfigurable antenna array and Synthetic Aperture Radar technique, which were applied for estimation of angular coordinates [7].

Infrared (IR), including active infrared laser radar and passive infrared, has been used in road vehicle acquisition, tracking, and especially for night vision. Infrared is available to operate in multiple lanes [1]. IR detecting techniques include extracting histograms of oriented gradient features and local binary pattern features, and concatenating to form classification features [8]. IR technique can be applied to detect both vehicles and pedestrians on road. However, infrared sensors may reduce vehicle sensitivity in bad weather conditions, like rain, fog and snow [1].

Cameras capture passing vehicle's location, speed and shapes in images and videos. Road traffic images contain rich information in wide area. Vehicle image detecting techniques can be used in multiple lanes and multiple zones. Weather conditions and day-to-night transition may heavily affect the performance [1]. Street lighting is required to assist video image recording at night time for obtaining reliable signals [1]. In literature, vehicle's parameters such as length, height and width dimensions were extracted and these features are used to classify vehicle types [9].

Magnetic sensors measure the magnetic field. Magnetic sensing technologies include: squid, fiber-optic, optical pumped, nuclear procession, search-coil, anisotropic magneto-resistive, flux-gate, and so on [10]. These sensors detect different magnetic field range. The impact of a vehicle passing or stopping causes a change to the earth magnetic field within the range of 1 microgauss to 10 gauss [10]. Comparing with other types of magnetic field sensing technologies in range and cost, Anisotropic Magneto-Resistive (AMR) sensors are able to work in this range of magnetic field changes for practical applications.

Signal analysis of magnetic field measurement and classifying into signal shape patterns has been an effective approach. In Sing Yiu et al.'s approach [11], three-axis magnetic vectors were analyzed separately in magnitude. The magnitudes of signals in the x, y and z in time series were classified into a number of patterns. These patterns illustrated the shape of hills for each type of vehicles. Using the hill pattern approach, Saowaluck et al. [12] extracted features of normalized vehicle magnetic length, average energy, number of peaks from hill patterns. Their classification types include motorcycles, cars, pickups, vans, and buses.

An integrated approach was developed using magnetic sensor and DGPS by Taghvaeeym and Rajamani [13]. In [13], two magnetic sensors were used. DGPS measured the speed of vehicles to aid the magnetic sensing. The vehicle classification was based on magnetic length and estimate of the average vertical magnetic height of the vehicle. Vehicle length was computed by using the vehicle presence time and vehicle speed.

Using a single AMR sensor, Yang and Lei [14] detected vehicles in a single lane by using sensor measurement when vehicle passing the road sensing area. The following features were extracted from measured signals for classification: signal duration, signal energy, average signal of signal, ratio of positive and average energy of X-axis signal, and ratio of positive and average energy of Y-axis signal. X-axis and Y-axis of the magnetic sensor were installed parallel to the earth surface. Z-axis was vertically installed. The types were classified into motorcycles, two-box cars, saloon cars, and sport utility vehicles in [14].

Among these approaches, the vehicle detection and classification had been developed as prototypes. In AMR sensor-related systems, AMR sensors were installed on roadside, under the surface of road, used a single sensor, or applied multiple sensors as a sensor network. These impact the factors of measured signal strength for detecting accuracy, cost of installation and maintenance. Application in deployment has not been commercialized in large scale yet due to these impact factors. Further research of approaches is needed to achieving reliable detection and classification results while reducing the cost caused by sensor installation and maintenance.

Compared with different types of sensors, e.g. radar, optical images/videos and Infrared, AMR sensor has three main advantages. 1) The AMR is the overall systems low cost and smaller size due to high sensitivity, and they still maintain reliability and quality. 2) AMR sensors have high sensitivity and flexibility; therefore, they are placed further away from the magnet. This allows the AMR sensor to be installed where it is needed for the optimal performance. And, 3) the most advantage of these solid-state devices are their durability and immunity to shock and vibration. They record magnetic signals in a stable fashion that is not influenced by different weather conditions.

In our research, considering the cost of installation and maintenance, we use a single AMR magnetic sensor to install on roadside. Our approach is proposed for Australia road environment. The types of vehicles in Australia road traffic are typically sedan, van, truck and bus. We analyze these vehicle types by using measured earth magnetic field signal changes in time domain, when vehicle passes our sensing area. We explore vehicle identification and classification by extending audio signal analysis approach. The sensor measurements of magnetic field are processed by signal feature extraction and vector quantization for vehicle type classification. Compared with Yang and Lei's work, we target vehicle types which are suitable to Australia road traffic. Our method of feature extraction and classification outperforms the method proposed in [14] 1% on average classification accuracy.

## III. EXPERIMENT DESIGN USING MAGNETIC SENSOR IN ROAD TRAFFIC

In our experiments, an AMR magnetic sensor is installed on road side to collect data of a single lane. The distance between the sensor and passing vehicles is 60 centimeters. The roadside sensor is able to detect one vehicle on one lane in our

experiment. When vehicle passes the sensing area, the magnetic field in that area will change and cause the magnetic measurement changes. These changes are displayed as a signal wave in measurement. From the observation of vehicle types on road, we classify and analyze road vehicles using four types: sedan, van, truck, and bus. When these vehicles pass the experiment spot, the magnetic field measurements display signal changes as the form of waves. We have applied dynamic time warping (DTW) to select the most representative samples from each vehicle type. Figure 1, 2, 3, 4 illustrate the magnetic field changes in one dimension for these types of vehicles.

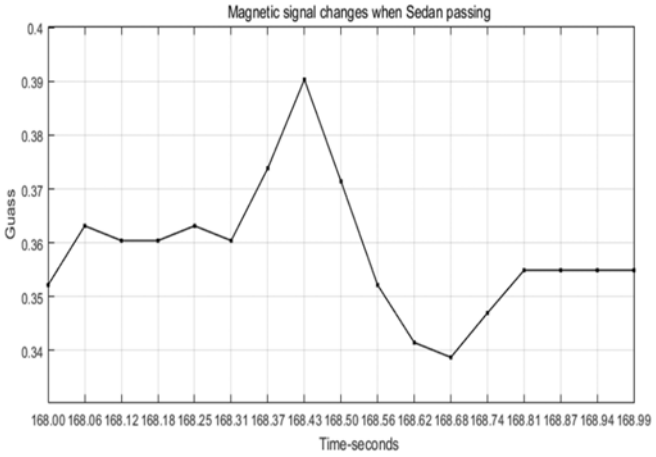


Fig. 1. Magnetic sensor measurement of Sedan signal

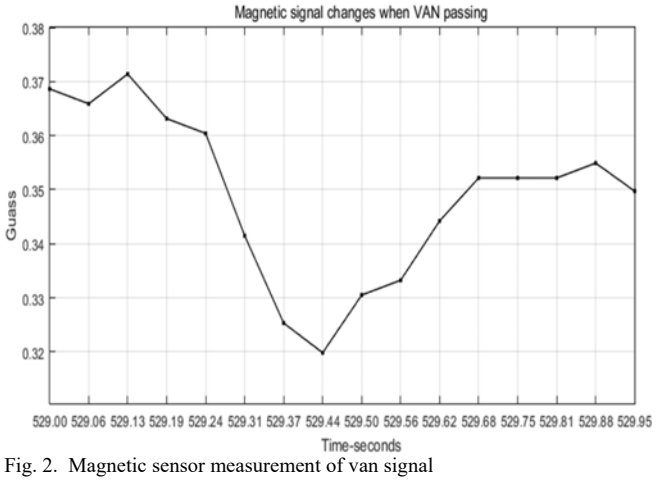


Fig. 2. Magnetic sensor measurement of van signal

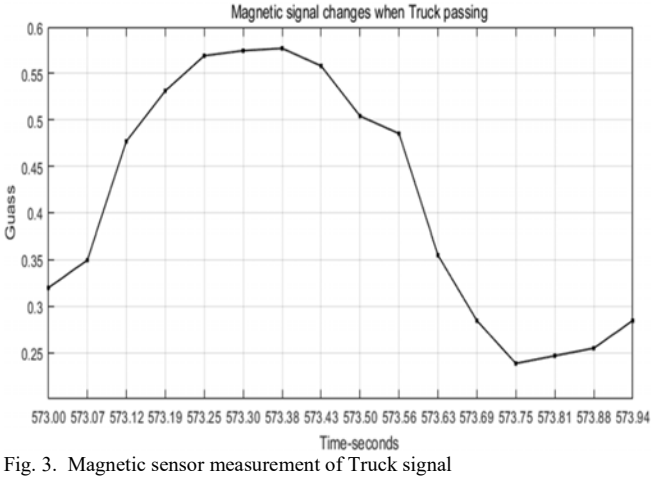


Fig. 3. Magnetic sensor measurement of Truck signal

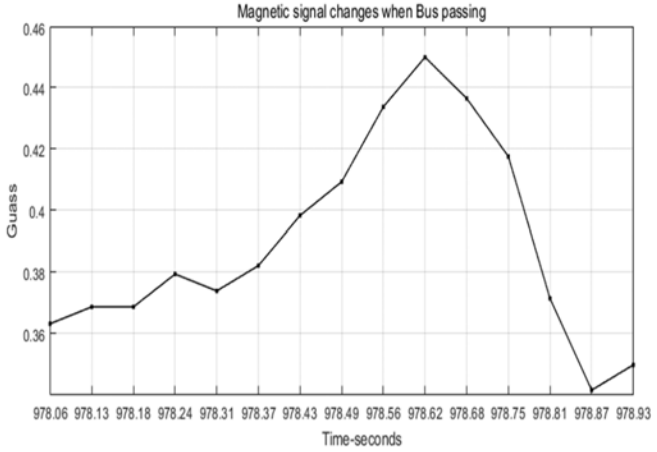


Fig. 4. Magnetic sensor measurement of Bus signal

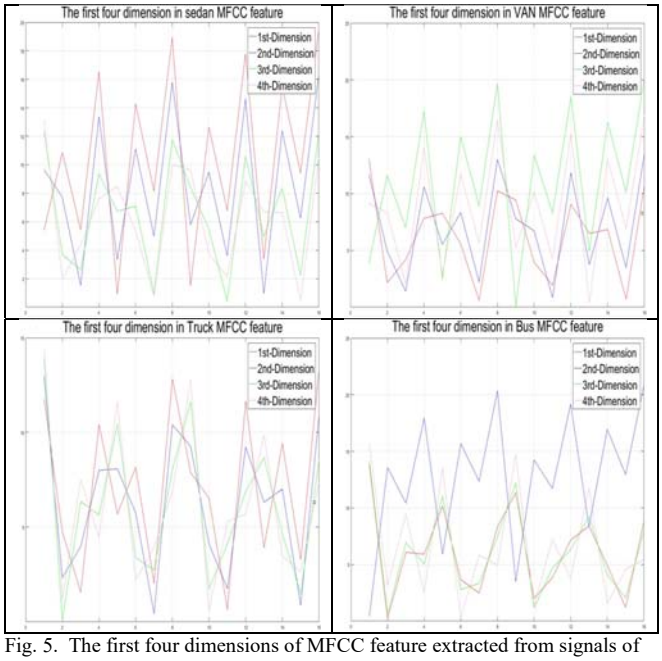


Fig. 5. The first four dimensions of MFCC feature extracted from signals of four different vehicle types

From the experiments, we found that magnetic signal wave and audio wave display similar characteristics, such as reflection, refraction, intervene, measurement data and

diffraction. In time domain and frequency domain, the speed, length, and frequency of signal waves have certain relationship for both magnetic wave and audio wave. In our research, we explore filtering raw magnetic measurement signals as well as the signal feature extraction to analyze magnetic field signal features.

In this paper, we present a road vehicle detection and classification approach using magnetic sensor and magnetic signal feature extraction and classification. In order to reduce the deployment, interruption of road traffic and maintenance cost, we apply a road-side magnetic sensor to detect the vehicles. The magnetic signal processing approach extended MFCC to extract the magnetic signal feature and classify the feature to categorize five types, as shown in Figure 6. In our experiments, the signal types are: sedan, van, truck, bus and non-vehicle. Figure 5 shows the first four dimensions of MFCC extracted from the signature signal of four different vehicle types. Usually, when there is no vehicle in measurement area, the basic output signal from magnetic sensor is the earth magnetic field with environment noises. The non-vehicle can also include passengers, bicycles and motors and the earth magnetic field with environment noises. Since the signal sample length is set as one second, the number of non-vehicle samples is the number of seconds that non-vehicle signal lasts.

## IV. VEHICLE CLASSIFICATION ALGORITHM

In our research, we extract Mel Frequency Cepstral Coefficients (MFCC) feature from signals and apply Vector Quantization (VQ) to classify magnetic field measurement data for passing vehicles. In order to efficiently model the probability density functions, we use Dynamic Time Warping (DTW) to filter the raw measurement signals to prepare training data for VQ. MFCC has been proved to be one of the robust and widely used features to analyze the characteristic of audio signals [15, 16]. Vector Quantization is a classifier to compare the distance in vectors. VQ transforms several scalar data into one vector data, and quantizes whole vector space [17].

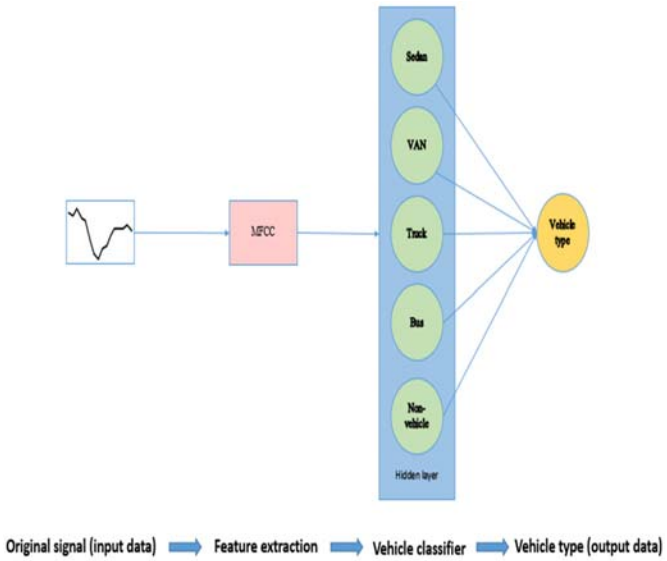


Fig. 6. Vehicle magnetic feature extraction and classification process

In identification and classification of vehicle signals, we filter the raw magnetic field measurement signals and extract relative features, and then label the features to different types of vehicles. The method is presented below.

### *A. Training sample selection by dynamic time warping selection of magnetic measurement signal*

As we all know, for effective machine learning to occur, it is important to select representative positive training samples. Collected magnetic signals can be very raw due to noisy introduced by environmental condition. (i.e. pedestrian, road work, train/tram noise and track maintenance) In order to accurately model the probability density function for each type of vehicle, we introduce sample selection to make sure training data efficiently represent the characteristics of each vehicle type. Since magnetic signals are complex series with the shift and stretching of amplitude, dynamic time warping (DTW) is applied in our research to measure similarity among signals. In some boundary and temporal consistency constrains, DTW is a point to point method and it can obtain a global optimal solution through cost matrix [18, 19].

For each vehicle class, assuming we have n magnetic signals $S = \{s_1, s_2, s_3 \cdots s_n\}$. Any two magnetic signals of one category are compared with each other. Figure 7 shows an example of comparison of two van sample pairs. We apply 16 sampling points. Each point has been compared between two magnetic signals.

Assuming $s_w = \{x_i\}_{i=1}^{16}$ and $s_u = \{y_j\}_{j=1}^{16}$ are the two signals in $S$. When $\mathrm{u} \neq \mathrm{w}$, $\mathrm{u} = 1, \ldots, \mathrm{n}$, $\mathrm{w} = 1, \ldots, \mathrm{n}$, $x_i, i = 1, \ldots, 16$ and $y_j, j = 1, \ldots, 16$ represent the sample points of two magnetic signals, $s_w$ and $s_u$. $\mathrm{DTW}(s_w, s_u)$ is used to present the DTW distance between $s_w$ and $s_u$, which can be calculated by the following equation (1).

$$\mathrm{DTW}(s_w, s_u) = \sum_{i=1}^{i} \sum_{j=1}^{j} min(d(x_{i-1}, y_j), d(x_i, y_{j-1}), d(x_{i-1}, y_{j-1})). \quad (1)$$

Where $d(x_i, \langle\rangle) = \infty$, $d(\langle\rangle, y_j) = \infty$ and $d(\langle\rangle, \langle\rangle) = 0$. The $\langle\rangle$ indicates empty series. The $d(x_i, y_j)$ indicates the distance between two points $x_i$ and $y_j$, which can be represented by Euclidean Distance.

The $D = \{D_1, D_2, D_3 \ldots D_{n-1}\}$ describes a set of DTW distance that each magnetic signal compared with the rest signals within the same class, as demonstrated below:

$$\begin{aligned} D_1 &= \{DTW_{1,2}, DTW_{1,3}, \cdots, DTW_{1,n}\} \\ D_2 &= \{DTW_{2,1}, DTW_{2,3}, \cdots, DTW_{2,n}\} \\ &\vdots \\ D_{n-1} &= \{DTW_{n,1}, DTW_{n,2}, \cdots, DTW_{n,n-1}\}. \end{aligned} \quad (2)$$

The average distance between each magnetic signal to the rest within the same class can be calculated as follows:

$$\overline{D_1} = \frac{1}{n-1}\left(DTW_{1,2} + DTW_{1,3} + \cdots + DTW_{1,n}\right)$$

$$\overline{D_2} = \frac{1}{n-1}\left(DTW_{2,1} + DTW_{2,3} + \cdots + DTW_{2,n}\right)$$
$$\vdots$$
$$\overline{D_{n-1}} = \frac{1}{n-1}\left(DTW_{n,1} + DTW_{n,2} + \cdots + DTW_{n,n-1}\right) \quad (3)$$

The equation (3) can be further summarized as

$$\overline{D_p} = \frac{1}{n-1}\left(\sum_{\substack{m=1,\ldots,n \\ m\neq p}} DTW_{p,m}, p = 1, \ldots, n-1\right)$$

$$D_r = \underset{p}{\operatorname{argmin}}\left\{\overline{D_p}, p = 1, \ldots, n-1\right\}. \quad (4)$$

We then select $S_r$ as the signature magnetic signal of the class where $S_r$ belongs to. For four vehicle classes, we can acquire four signature signals, which is showed in Figure 1, 2, 3, 4.

In order to select training samples of each vehicle class, we calculate the DTW distance of each sample in that class to the signature signal of that class and select samples with DTW distance no greater than 2 as training samples. The number of training samples of each vehicle class are listed in the APPENDIX. Fig. 7 shows an example, which is a van signal compared with its signature signal. The DTW distance between these two signals is 0.167847.

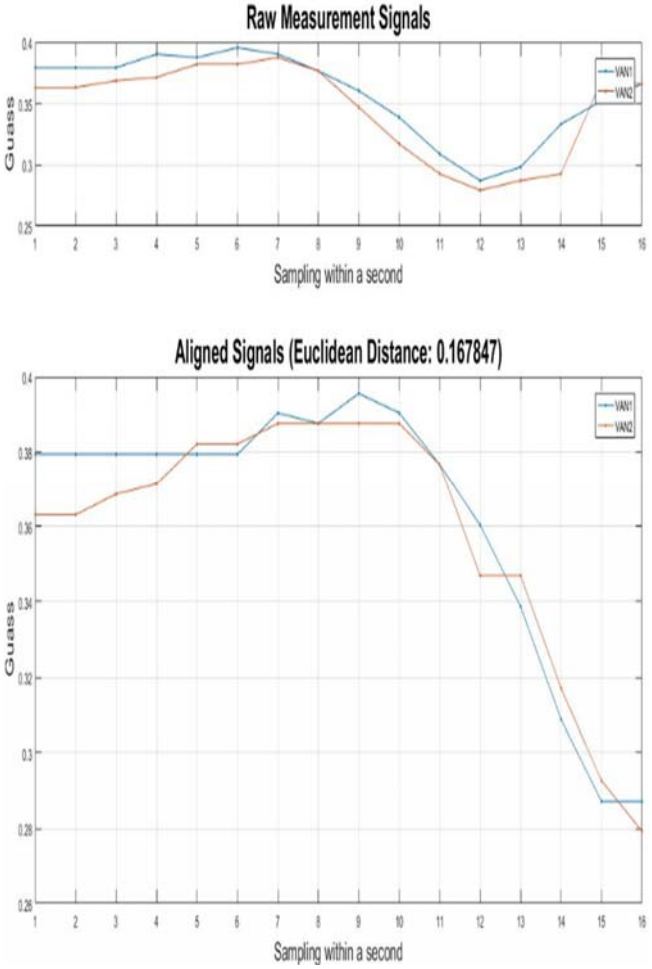


Fig. 7. An example of a van signal compared with its signature signal by DTW

### B. *Magnetic feature extraction process*

The process flow of magnetic field features extraction is as Figure 8. Each step of the process is presented in this section.

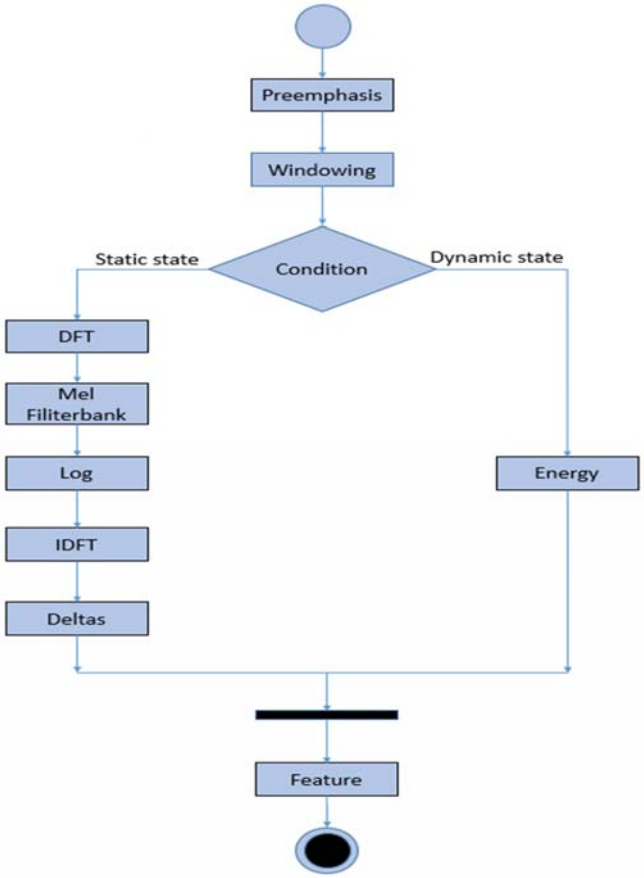


Fig. 8. Magnetic measurement feature extraction

**Preemphasis.** The first step of magnetic signal feature extraction is "preemphasis". This step improves the energy in high frequencies and balances the energy from lower and higher frequencies. In the time domain, the filter equation is as below:

$$y[n] = x[n] - \alpha x[n-1]. \quad (5)$$

where, $n$ is the time, x[n] is the input signal, and $0.9 \leq \alpha \leq 1$.

**Windowing.** In the second step "Windowing", we extract signal feature from a small window of signal. The windowing process is performed using signal value and window value. If the value of the signal at time $n$ is $s[n]$, the value of the window at time $n$ is $w[n]$, the signal value y[n] of this windowing process is presented as the following equation:

$$y[n] = w[n]s[n]. \quad (6)$$

In order to shrink the values of the signal toward zero at the window boundaries and avoid discontinuities, we define two windowing functions: "Rectangular" and "Hamming".

**Rectangular.** We set the window to 1 when signal time $n$ is between 0 and $L$-1, $L$ is the length of the frame of the signal. In

another time period, we set window to 0 [15, 16].

$$\mathrm{w}[[\mathrm{n}] = \begin{cases} 1 & 0 \le n \le L-1 \\ 0 & otherwise \end{cases}. \quad (7)$$

**Hamming.** Hamming window is the goal to extract the spectral features, not from the entire signal, it can extract spectral features from a small window of signal [15, 16].

$$\mathrm{w}[\mathrm{n}] = \begin{cases} 0.54 - 0.46\cos\frac{2\pi n}{L} & 0 \le n \le L-1 \\ 0 & otherwise \end{cases}. \quad (8)$$

After the "Windowing" process, the distributed frames will result in two states: dynamic state and static state. The feature extracting process will go through two different flows as in Figure 8. After "Windowing" processing, there is a condition to process each frame in magnetic feature and here are two steps including dynamic and static site, due to the reason of each frame in "Windowing".

The windowing process includes "frame shift" and "frame size". In the frame state, there are two conditions: *dynamic state* and *static state* to resolve this issue. The *dynamic* processing is caused by frame shift that is 10ms, while the *static* state is frame size, which is 25ms. Therefore, the total feature is the data of dynamic and static.

***Static state:***

**Discrete Fourier Transform (DFT).** For static frame condition, the third step is Discrete Fourier Transform (DFT). We extract magnetic information for windowed signal. We calculate how much energy the signal contains at different frequency bands. DFT is defined as:

$$x[k] = \sum_{n=0}^{N-1} x[n]e^{j\theta}. \quad (9)$$

where *k* and *N* are the sequence of frame and discrete frequency bands respectively. The e, and $\theta$ are presented in Euler's formula as below:

$$e^{j\theta} = \cos\theta + j\sin\theta. \quad (10)$$

Where, $\theta = -2\frac{\pi}{N}kn$.

**Mel Filter Bank.** The next steps of feature extraction are "Mel Filter Bank" and "Log Processing" to reduce to lower amplitudes. This is computed using:

$$mel(f) = 1127In^{(1+\frac{f}{700})}. \quad (11)$$

where *f* is the frequency of the input signal.

The final steps are "Inverse Discrete Fourier Transform" (IDFT) and "Deltas" and "Energy": therefore, the magnetic feature include Cepstrum, Deltas and Energy.

**Inverse Discrete Fourier Transform (IDFT).** IDFT is computed using the following equations:

$$c[n] = \sum_{n=0}^{N-1} log^{(|\sum_{n=0}^{N-1} x[n]e^{-j\frac{2\pi}{N}kn}|)} e^{j\frac{2\pi}{N}kn}. \quad (12)$$

where *c* is the cepstrum of magnetic feature.

**Delta.** In Delta stage, we compute the gap cepstrum (delta). Delta is defined as the value of average of current cepstrum and the cepstrum of next time. Delta *d* is computed as below.

$$d(t) = \frac{c(t+1)-c(t)}{2}. \quad (13)$$

**Double delta** is defined as:

$$z(t) = \frac{c(t+1)-c(t-1)}{2}. \quad (14)$$

***Dynamic state:***

For the dynamic state frames after "Windowing", we start "Energy" process as in Figure 8.

**Energy.** *Energy* is computed using the energy of the frame between two time points $t_1$ and $t_2$. We calculate Energy of cepstrum *c*, delta *d* and double delta *z*.

$$Energy = \sum_{t=t_1}^{t_2} x^2[t]. \quad (15)$$

**Feature.** For both process flows for dynamic state and static state as in Figure 8, the final features are integrated. Magnetic feature is presented using integration of cepstrum *c*, delta *d*, double delta *z* and Energy, as in Equations 12, 13, 14 and 15. Vehicle magnetic features are consequently extracted and represented in this process.

### *C. Vehicle classification process*

To classify magnetic sensor signals for vehicle types, we transform several scalar magnetic measurement data into one vector. We design this vector containing cepstrum *c*, *Energy*, and the gap cepstrum *d*, which are extracted from the vehicle magnetic feature extraction process.

A vector space is quantized using all magnetic feature vectors. We compress data and store this feature information in magnetic vector space [20].

We design a 3-dimensional classification model to present the distribution of vehicle types as in Figure 9.

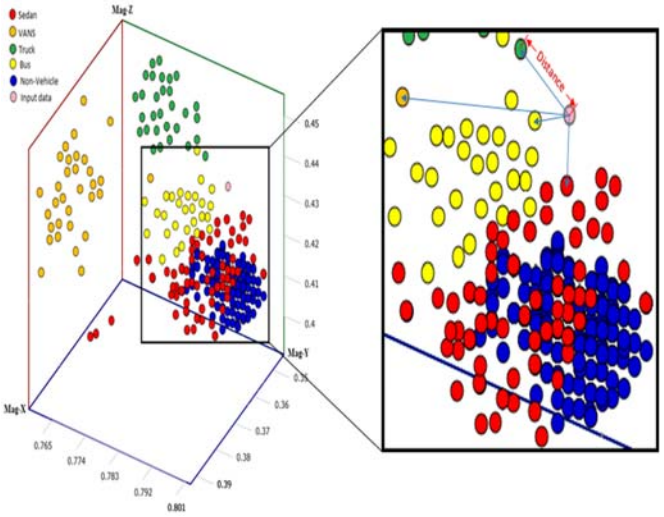


Fig. 9. Distribution of vehicles on 3-dimensional classification algorithm

In this distribution 3-dimension model (magnetic-x, magnetic-y, magnetic-z), we design three axes as the coordinate. The coordinate displays the different vehicles in the region. We uniquely represent each color circle by this coordinate. In this case, we design sedan as red circle, vans as orange circle, truck as dark red circle, bus as yellow circle, none-vehicle as blue circle and input data as pink circle in Figure 9. For example, we design the coordinate [0.352, 0.412, 0.786] to allocate the position of one passing sedan in this distribution. The VQ algorithm compares the distance between input data (pink circle) and others vehicles (red circle, orange circle, dark red circle, yellow circle, blue circle). If the distance between the input data (pink circle) and sedan (red circle) is the shortest, the input signal is labeled as a sedan. Similarly, each input signal has corresponding vehicle label in this 3-dimension space.

The classification algorithm is roughly described as follows. Given $M$ as the number of training samples, the training data set can be represented as $X = \{x_m, m = 1, \dots, M\}$. For each training sample in the training set, $x_m = \{x_{m,1}, x_{m,2}, \dots, x_{m,k}\}$, where $k$ represents the dimension number of a feature vector used to represent each sample. Divide the classification feature space to $N$ parts, i.e. $N$ classes. In our case, $N$ =5 to indicate five pre-defined vehicle classes. For each vehicle class n, a code vector $c_n = \{c_{n,1}, c_{n,2}, \dots, c_{n,k}\}$, which is the feature vector of the centroid point of that class. Therefore, in our case, the codebook of classification space can be represented as $C = \{c_n, n = 1, \dots, 5\}$. $S_n$ is the encoding region including $c_n$. We set partition of the space $P = \{S_n, n = 1, \dots, 5\}$. If $x_m$ is in $S_n$ area, $x_m$ can be quantized as $c_n$: $Q(x_m) = c_n$.

The average distortion $D_{ave}$ can be computed using

$$D_{ave} = \frac{1}{Mk}\sum_{m=1}^{M}|x_m - Q(x_m)|^2. \quad (16)$$

We design optimality criteria using "Nearest Neighbor Condition" and "Centroid Condition".

These criteria are presented as follows:

"**Nearest Neighbor Condition**":

$$S_n = \{x: |x - c_n|^2 \le |x - c_{n'}|^2 \ \forall n' = 1,2, \dots, N\}. \quad (17)$$

The vectors standing on boundary can be chosen to certain region $S_n$.

"**Centroid Condition**":

$$c_n = \frac{\sum x_m \in s_n^{X_m}}{\sum x_m \in s_n^1} \ n = 1,2, \dots, N. \quad (18)$$

If the transformed vehicle magnetic vector meets the both "Nearest Neighbor Condition" and "Centroid Condition", then the magnetic vector can be classified into that vehicle type.

## V. ANALYSIS OF VEHICLE CLASSIFICATION EXPERIMENT RESULTS

We perform experiments for vehicle type classification, i.e. classifying signals into five classes including sedan, van, truck, bus and non-vehicle, based on features extracted from each signal. "non-vehicle" type is defined for magnetic signals when vehicles are absent.

### *A. Classification with rough training data and cross-validation*

We separate magnetic measurement data into two sets: training data set and testing data set. Experiments are set up in three groups. In Experiment Group 1, we set up 2/3 of entire data (87 sedans, 76 vans, 82 trucks, 71 buses and 96 non-vehicle signals) as training data and the rest 1/3 data as testing data. In Experiment Group 2, we set up 3/4 as training data and 1/4 as testing data. The last group 3, we set up 4/5 as training data and 1/5 as testing data.

The cross-validation is an approach to generalize the classification result to an independent data set. In our approach, we apply K-fold approaches [21]. K is set up as 3, 4 and 5 respectively for different experiment groups. For Group 1 of 3-fold, we firstly divided the entire experimental data into three partitions, each of which had 1/3 of the total data. One of the partitions was picked up as testing data. The data in the other two partitions were training data. Then, the second partition was used for testing and the rest two partitions were for training. After that, the third 1/3 data were for testing, and the rest 2/3 data were for training. At the end, the three times accuracies are averaged as the classification accuracy for 3-fold cross-validation. For Group 2 of 4-fold, we divided the whole data set into 4 partitions. Each partition was in turn used for testing and the rest were for training. Then, the average accuracy was calculated. For Group 3, i.e. 5-fold, the data were divided into 5 partitions for experiments.

Cross-validation classification results of each experimental group are listed in Table 1. The number of training samples and testing samples are also listed. Please note, when the total number of samples cannot be divisible by K, the number of training and testing samples can be slightly different for each cross-validation run of the same experiment group. It is obvious

that, the less the testing data, i.e. the more the training data, the higher the classification accuracy.

| | | Sedan | Van | Truck | Bus | Non |
|---|---|---|---|---|---|---|
| No. total samples | | 87 | 76 | 82 | 71 | 96 |
| Group 1 | No. Train | 58 | 51/0 | 55/4 | 47/8 | 64 |
| | No. Test | 29 | 25/6 | 27/8 | 24/3 | 32 |
| | Accuracy | 56% | 67% | 65% | 71% | 61% |
| Group 2 | No. Train | 65/6 | 57 | 61/3 | 53/4 | 72 |
| | No. Test | 22 | 19 | 21/19 | 18/7 | 24 |
| | Accuracy | 61% | 70% | 67% | 74% | 65% |
| Group 3 | No. Train | 70/68 | 61/0 | 66/4 | 57/6 | 77/6 |
| | No. Test | 17/9 | 15/6 | 16/8 | 14/5 | 19/20 |
| | Accuracy | 67% | 72% | 68% | 77% | 71% |

Table 1. Cross-validation accuracies of three groups with rough training data

### *B. Classification with DTW selected training data and cross-validation*

As we known, training sample selection is vital for effective machine learning to occur. Different from experiments proposed in V.A, in order to improve the classification performance, all training data has been further selected by applying Dynamic Time Warping (DTW). For each vehicle type, we set DTW$= 2$ as a threshold value to select training data. If $\mathrm{DTW}(s_w, s_r) < 2$, then $s_w$ will be selected for training. As discussed in Section IV.A, $s_r$ is the signature in a particular vehicle class and $s_w$, $w = 1, \ldots, \mathrm{n}, w \neq \mathrm{r}$, indicates the rest signals in the same class. The numbers of training data used for different sets of experiments are listed in the APPENDIX.

Table 2 summarizes the cross-validation accuracies of three groups with DTW selected training data. We also list the number of training and test samples in the table. When the total number of samples cannot be divisible by K, the number of testing data can be slightly different for each cross-validation run of the same experiment group. Detailed experimental results of cross-validation runs can be found in VII. Appendix.

| | | Sedan | Van | Truck | Bus | Non |
|---|---|---|---|---|---|---|
| No. total samples | | 87 | 76 | 82 | 71 | 96 |
| Group 1 | No. Train | 50 | 46 | 50 | 42 | 57 |
| | No. Test | 29 | 25/6 | 27/8 | 24/3 | 32 |
| | Accuracy | 84% | 85% | 83% | 91% | 89% |
| Group 2 | No. Train | 60 | 51 | 55 | 48 | 65 |
| | No. Test | 22 | 19 | 21/19 | 18/7 | 24 |
| | Accuracy | 90% | 88% | 86% | 97% | 95% |
| Group 3 | No. Train | 64 | 53 | 58 | 51 | 68 |
| | No. Test | 17/9 | 15/6 | 16/8 | 14/5 | 19/20 |
| | Accuracy | 93% | 91% | 93% | 99% | 97% |

Table 2. Cross-validation accuracies of three groups with DTW selected training data

Compared Table 2 with Table 1, we can find that the classification performance was improved significantly by selecting efficient training samples. DTW, as a filter, made a great contribution to increasing classification accuracy.

## VI. CONCLUSION

In this paper, we present a road vehicle identification and classification approach using magnetic sensing, magnetic signal feature extraction and classification. This approach is designed for analyzing road traffic in intelligent transportation systems.

Using this approach, the installation of magnetic sensor in roadside does not require interruption of road traffic. This reduces the deployment and maintenance cost.

Processing magnetic signals by extracting the features of MFCC and VQ based on classification can categorize five types of vehicle signals. Applying DTW to select efficient training samples can further improve the classification accuracy significantly.

As an initial research, we have set up distance between the sensor and passing vehicles as 60 centimeters. In our future studies, we will consider applying multiple sensors to monitor multiple lanes. Moreover, experiments can be carried out to investigate the effect of various distance between AMR sensor and passing vehicles.

## VII. APPENDIX

Detailed experimental results of cross-validation runs are listed as follows.

### *A. Classification with rough training data and cross-validation*

| | Sedan | Van | Truck | Bus | Non-vehicle |
|---|---|---|---|---|---|
| No. total | 87 | 76 | 82 | 71 | 96 |
| No. Train | 58 | 51 | 55 | 47 | 64 |
| No. Test | 29 | 25 | 27 | 24 | 32 |
| No. correct | 18 | 18 | 17 | 15 | 20 |
| Accuracy | 62% | 72% | 63% | 63% | 63% |

Table 3: Group 1 round 1 accuracy with rough training data (2/3 for training and 1/3 for testing)

| | Sedan | Van | Truck | Bus | Non-vehicle |
|---|---|---|---|---|---|
| No. total | 87 | 76 | 82 | 71 | 96 |
| No. Train | 58 | 51 | 55 | 47 | 64 |
| No. Test | 29 | 25 | 27 | 24 | 32 |
| No. correct | 16 | 17 | 17 | 16 | 20 |
| Accuracy | 55% | 68% | 63% | 67% | 63% |

Table 4: Group 1 round 2 accuracy with rough training data (2/3 for training and 1/3 for testing)

| | Sedan | Van | Truck | Bus | Non-vehicle |
|---|---|---|---|---|---|
| No. total | 87 | 76 | 82 | 71 | 96 |
| No. Train | 58 | 50 | 54 | 48 | 64 |
| No. Test | 29 | 26 | 28 | 23 | 32 |
| No. correct | 15 | 16 | 19 | 19 | 18 |
| Accuracy | 56% | 67% | 65% | 71% | 61% |

Table 5: Group 1 round 3 accuracy with rough training data (2/3 for training and 1/3 for testing)

| | Sedan | Van | Truck | Bus | Non-vehicle |
|---|---|---|---|---|---|
| No. total | 87 | 76 | 82 | 71 | 96 |
| No. Train | 65 | 57 | 61 | 53 | 72 |
| No. Test | 22 | 19 | 21 | 18 | 24 |
| No. correct | 13 | 13 | 14 | 12 | 16 |
| Accuracy | 59% | 68% | 67% | 68% | 67% |

Table 6: Group 2 round 1 accuracy with rough training data (3/4 for training and 1/4 for testing)

| | Sedan | Van | Truck | Bus | Non-vehicle |
|---|---|---|---|---|---|
| No. total | 87 | 76 | 82 | 71 | 96 |
| No. Train | 65 | 57 | 61 | 53 | 72 |
| No. Test | 22 | 19 | 21 | 18 | 24 |
| No. correct | 12 | 14 | 14 | 14 | 17 |
| Accuracy | 55% | 74% | 68% | 78% | 71% |

Table 7: Group 2 round 2 accuracy with rough training data (3/4 for training and 1/4 for testing)

| | Sedan | Van | Truck | Bus | Non-vehicle |
|---|---|---|---|---|---|
| No. total | 87 | 76 | 82 | 71 | 96 |
| No. Train | 65 | 57 | 61 | 53 | 72 |
| No. Test | 22 | 19 | 21 | 18 | 24 |
| No. correct | 15 | 13 | 15 | 13 | 15 |
| Accuracy | 68% | 68% | 71% | 72% | 63% |

Table 8: Group 2 round 3 accuracy with rough training data (3/4 for training and 1/4 for testing)

| | Sedan | Van | Truck | Bus | Non-vehicle |
|---|---|---|---|---|---|
| No. total | 87 | 76 | 82 | 71 | 96 |
| No. Train | 66 | 57 | 63 | 54 | 72 |
| No. Test | 21 | 19 | 19 | 17 | 24 |
| No. correct | 13 | 13 | 13 | 13 | 14 |
| Accuracy | 61% | 70% | 67% | 74% | 65% |

Table 9: Group 2 round 4 accuracy with rough training data (3/4 for training and 1/4 for testing)

| | Sedan | Van | Truck | Bus | Non-vehicle |
|---|---|---|---|---|---|
| No. total | 87 | 76 | 82 | 71 | 96 |
| No. Train | 70 | 61 | 66 | 57 | 77 |
| No. Test | 17 | 15 | 16 | 14 | 19 |
| No. correct | 12 | 11 | 11 | 12 | 15 |
| Accuracy | 71% | 73% | 68% | 86% | 79% |

Table 10. Group 3 round 1 accuracy with rough training data (4/5 for training and 1/5 for testing)

| | Sedan | Van | Truck | Bus | Non-vehicle |
|---|---|---|---|---|---|
| No. total | 87 | 76 | 82 | 71 | 96 |
| No. Train | 70 | 61 | 66 | 57 | 77 |
| No. Test | 17 | 15 | 16 | 14 | 19 |
| No. correct | 12 | 10 | 11 | 10 | 13 |
| Accuracy | 71% | 67% | 68% | 71% | 68% |

Table 11. Group 3 round 2 accuracy with rough training data (4/5 for training and 1/5 for testing)

| | Sedan | Van | Truck | Bus | Non-vehicle |
|---|---|---|---|---|---|
| No. total | 87 | 76 | 82 | 71 | 96 |
| No. Train | 70 | 61 | 66 | 57 | 77 |
| No. Test | 17 | 15 | 16 | 14 | 19 |
| No. correct | 11 | 11 | 10 | 12 | 14 |
| Accuracy | 65% | 73% | 62% | 86% | 74% |

Table 12. Group 3 round 3 accuracy with rough training data (4/5 for training and 1/5 for testing)

| | Sedan | Van | Truck | Bus | Non-vehicle |
|---|---|---|---|---|---|
| No. total | 87 | 76 | 82 | 71 | 96 |
| No. Train | 70 | 61 | 66 | 57 | 77 |
| No. Test | 17 | 15 | 16 | 14 | 19 |
| No. correct | 10 | 11 | 11 | 10 | 13 |
| Accuracy | 59% | 73% | 68% | 71% | 68% |

Table 13. Group 3 round 4 accuracy with rough training data (4/5 for training and 1/5 for testing)

| | Sedan | Van | Truck | Bus | Non-vehicle |
|---|---|---|---|---|---|
| No. total | 87 | 76 | 82 | 71 | 96 |
| No. Train | 68 | 60 | 64 | 56 | 76 |
| No. Test | 19 | 16 | 18 | 15 | 20 |
| No. correct | 10 | 12 | 13 | 11 | 13 |
| Accuracy | 68% | 75% | 72% | 73% | 65% |

Table 14. Group 3 round 5 accuracy with rough training data (4/5 for training and 1/5 for testing)

### *B. Classification with DTW selected training data and cross-validation*

| | Sedan | Van | Truck | Bus | Non-vehicle |
|---|---|---|---|---|---|
| No. total | 87 | 76 | 82 | 71 | 96 |
| No. Train | 50 | 46 | 50 | 42 | 57 |
| No. Test | 29 | 25 | 27 | 24 | 32 |
| No. correct | 23 | 22 | 22 | 20 | 27 |
| Accuracy | 79% | 88% | 81% | 83% | 84% |

Table 15. Group 1 round 1 accuracy with DTW selected training data (2/3 for training and 1/3 for testing)

| | Sedan | Van | Truck | Bus | Non-vehicle |
|---|---|---|---|---|---|
| No. total | 87 | 76 | 82 | 71 | 96 |
| No. Train | 50 | 46 | 50 | 42 | 57 |
| No. Test | 29 | 25 | 27 | 24 | 32 |
| No. correct | 23 | 20 | 25 | 22 | 29 |
| Accuracy | 79% | 80% | 93% | 92% | 91% |

Table 16. Group 1 round 2 accuracy with DTW selected training data (2/3 for training and 1/3 for testing)

| | Sedan | Van | Truck | Bus | Non-vehicle |
|---|---|---|---|---|---|
| No. total | 87 | 76 | 82 | 71 | 96 |
| No. Train | 50 | 46 | 50 | 42 | 57 |
| No. Test | 29 | 26 | 28 | 23 | 32 |
| No. correct | 27 | 23 | 21 | 22 | 29 |
| Accuracy | 93% | 88% | 75% | 96% | 91% |

Table 17. Group 1 round 3 accuracy with DTW selected training data (2/3 for training and 1/3 for testing)

| | Sedan | Van | Truck | Bus | Non-vehicle |
|---|---|---|---|---|---|
| No. total | 87 | 76 | 82 | 71 | 96 |
| No. Train | 60 | 51 | 55 | 48 | 65 |
| No. Test | 22 | 19 | 21 | 18 | 24 |
| No. correct | 19 | 16 | 19 | 18 | 24 |
| Accuracy | 86% | 84% | 90% | 100% | 100% |

Table 18. Group 2 round 1 accuracy with DTW selected training data (3/4 for training and 1/4 for testing)

| | Sedan | Van | Truck | Bus | Non-vehicle |
|---|---|---|---|---|---|
| No. total | 87 | 76 | 82 | 71 | 96 |
| No. Train | 60 | 51 | 55 | 48 | 65 |
| No. Test | 22 | 19 | 21 | 18 | 24 |
| No. correct | 19 | 17 | 19 | 17 | 22 |
| Accuracy | 86% | 89% | 90% | 94% | 92% |

Table 19. Group 2 round 2 accuracy with DTW selected training data (3/4 for training and 1/4 for testing)

| | Sedan | Van | Truck | Bus | Non-vehicle |
|---|---|---|---|---|---|
| No. total | 87 | 76 | 82 | 71 | 96 |
| No. Train | 60 | 51 | 55 | 48 | 65 |
| No. Test | 22 | 19 | 21 | 18 | 24 |
| No. correct | 21 | 17 | 17 | 18 | 21 |
| Accuracy | 95% | 89% | 81% | 100% | 88% |

Table 20. Group 2 round 3 accuracy with DTW selected training data (3/4 for training and 1/4 for testing)

| | Sedan | Van | Truck | Bus | Non-vehicle |
|---|---|---|---|---|---|
| No. total | 87 | 76 | 82 | 71 | 96 |
| No. Train | 60 | 51 | 55 | 48 | 65 |
| No. Test | 21 | 19 | 19 | 17 | 24 |
| No. correct | 19 | 17 | 16 | 16 | 24 |
| Accuracy | 90% | 89% | 84% | 94% | 100% |

Table 21. Group 2 round 4 accuracy with DTW selected training data (3/4 for training and 1/4 for testing)

| | Sedan | Van | Truck | Bus | Non-vehicle |
|---|---|---|---|---|---|
| No. total | 87 | 76 | 82 | 71 | 96 |
| No. Train | 64 | 53 | 58 | 51 | 68 |
| No. Test | 17 | 15 | 16 | 14 | 19 |
| No. correct | 15 | 13 | 15 | 14 | 19 |
| Accuracy | 88% | 87% | 94% | 100% | 100% |

Table 22. Group 3 round 1 accuracy with DTW selected training data (4/5 for training and 1/5 for testing)

| | Sedan | Van | Truck | Bus | Non-vehicle |
|---|---|---|---|---|---|
| No. total | 87 | 76 | 82 | 71 | 96 |
| No. Train | 64 | 53 | 58 | 51 | 68 |
| No. Test | 17 | 15 | 16 | 14 | 19 |
| No. correct | 16 | 13 | 14 | 14 | 18 |
| Accuracy | 94% | 87% | 88% | 100% | 95% |

Table 23. Group 3 round 2 accuracy with DTW selected training data (4/5 for training and 1/5 for testing)

| | Sedan | Van | Truck | Bus | Non-vehicle |
|---|---|---|---|---|---|
| No. total | 87 | 76 | 82 | 71 | 96 |
| No. Train | 64 | 53 | 58 | 51 | 68 |
| No. Test | 17 | 15 | 16 | 14 | 19 |
| No. correct | 16 | 14 | 16 | 14 | 17 |
| Accuracy | 94% | 93% | 100% | 100% | 89% |

Table 24. Group 3 round 3 accuracy with DTW selected training data (4/5 for training and 1/5 for testing)

| | Sedan | Van | Truck | Bus | Non-vehicle |
|---|---|---|---|---|---|
| No. total | 87 | 76 | 82 | 71 | 96 |
| No. Train | 64 | 53 | 58 | 51 | 68 |
| No. Test | 17 | 15 | 16 | 14 | 19 |
| No. correct | 16 | 14 | 15 | 13 | 19 |
| Accuracy | 94% | 93% | 94% | 93% | 100% |

Table 25. Group 3 round 4 accuracy with DTW selected training data (4/5 for training and 1/5 for testing)

| | Sedan | Van | Truck | Bus | Non-vehicle |
|---|---|---|---|---|---|
| No. total | 87 | 76 | 82 | 71 | 96 |
| No. Train | 64 | 53 | 58 | 51 | 68 |
| No. Test | 19 | 16 | 18 | 15 | 20 |
| No. correct | 18 | 15 | 16 | 15 | 20 |
| Accuracy | 95% | 94% | 89% | 100% | 100% |

Table 26. Group 3 round 5 accuracy with DTW selected training data (4/5 for training and 1/5 for testing)

## REFERENCES


[1] US Department of Transportation (2006) "Federal Highway Administration Research and Technology Coordinating, Developing Highway Transportation Innovations" May 2006

[2] Mazarakis Georgios and Avaritsiotis (2007) "Vehicle classification in sensor networks using time-domain signal processing and neural networks", Microprocessors and MICROSYSTEMS, Vol 31. pp 381-392, Feb. 2007

[3] Yong-Kul Ki and Doo-Kwon Baik (2006) "Vehicle-classification algorithm for single-loop detectors using neural networks", IEEE Trans. On Vehicle Technology, Vol. 55, No. 6, pp 1704-1711, Nov. 2006

[4] Bajaj P, Sharma P, and Deshmukh, "Bajaj, Preeti, Prashant Sharma, and Amol Deshmukh.(2007) "Vehicle Classification for Single Loop Detector with Neural Genetic Controller: A Design Approach." Intelligent Transportation Systems Conference, 2007. ITSC 2007. IEEE.

[5] Gajda J. and Stencel M.(2014) "A highly selective vehicle classification utilizing dual-loop inductive detector ", Metrology and measurement systems, 2014, 21 (3), pp 473-484

[6] Roe H. and Hobson GS. (1992) "Improved discrimination of microwave vehicle profiles", IEEE MTT-S International Microwave Symposium Digest 1992, 2:717-720 Vol 2.4

[7] Ignacio Llamas-Garro, Konstantin Lukin, Marcos T. de Melo; Jung-Mu Kim, (2016) "Frequency and angular estimation of detected microwave

source using aerial vehicles", 2016 IEEE MTT-S Latin America Microwave Conference (LAMC), Poerto Vallarta, Mexico.

[8] Hurney Patrick, Waidron Peter, Morgan Fearghal, Jone Edward, Glavin Martin (2015) Night-time pedestrian classification with histograms of oriented gradients-local binary patterns vectors', IEEE Transactions on Intelligent Transportation Systems. 2015, Vol. 9, Issue 1.

[9] Shi, Shengli, Zhong Qin, and Jianmin Xu (2007) "Robust algorithm of vehicle classification." Software Engineering, Artificial Intelligence, Networking, and Parallel/Distributed Computing, 2007. SNPD 2007. Eighth ACIS International Conference on. Vol. 3. IEEE, 2007.

[10] Caruso, Michael J., and Lucky S. Withanawasam. (1999) "Vehicle detection and compass applications using AMR magnetic sensors." Sensors Expo Proceedings. Vol. 477. 1999.

[11] Cheung, Sing, et al. (2005) "Traffic measurement and vehicle classification with single magnetic sensor." Transportation research record: journal of the transportation research board 1917 (2005): 173-181.

[12] Keawkamnerd, Saowaluck, Jatuporn Chinrungrueng, and Chaipat Jaruchart (2008) "Vehicle classification with low computation magnetic sensor." ITS Telecommunications, 2008. ITST 2008. 8th International Conference on. IEEE, 2008.

[13] Taghvaeeym S. and Rajamani R. (2014) "Portable roadside sensors for vehicle counting, classification, and speed measurement", IEEE Transactions on Intelligent Transportation Systems, Vol. 15, No. 1, 2014

[14] Yang Bo and Lei Yiqun, (2015) "Vehicle detection and classification for low-speed congested traffic with anisotropic magnetoresistive sensor', IEEE Sensors Journal, Vol. 15, No. 2, Feb. 2015.

[15] Ma, Z., Yu, H., Tan, Z. and Guo, J. (2016). Text-Independent Speaker Identification Using the Histogram Transform Model. IEEE Access, 4, pp.9733-9739.

[16] Al-Ali, A., Dean, D., Senadji, B., Chandran, V. and Naik, G. (2017). Enhanced Forensic Speaker Verification Using a Combination of DWT and MFCC Feature Warping in the Presence of Noise and Reverberation Conditions. IEEE Access, 5, pp.15400-15413.

[17] S. Singh, and E. Rajan (2011) "Vector Quantization approach for speaker recognition using MFCC and inverted MFCC", International Journal of Computer Applications, Vol. 17, No. 1, Mar 2011.

[18] F. Petitjean, G. Forestier, G Webb, A Nicholson, Y. Chen, and E. Keogh. Dynamic time warping averaging of time series allows faster and more accurate classification. In ICDM, 2014.

[19] L. Ye and E. Keogh. Time series shapelets: a new primitive for data mining. In SIGKDD, pages 947–956. ACM, 2009.

[20] Gray, Robert. (1984) "Vector quantization." IEEE ASSP Magazine 1.2 (1984): 4-29.

[21] Gu, B., Sheng, V., Tay, K., Romano, W. and Li, S. (2017). Cross Validation Through Two-Dimensional Solution Surface for Cost-Sensitive SVM. IEEE Transactions on Pattern Analysis and Machine Intelligence, 39(6), PP.1103-1121.